9 Surgery of the Cranio-Vertebral Junction: Image Guidance, Navigation, and Augmented Reality

Philippe Bijlenga and Max Jägersberg

9.1 Introduction

Safety, efficacy, and accessibility of surgery are major aims identified by the World Health Organization to improve global care. Safety is the power to avoid injury. Efficacy is the power to cure. Accessibility is the power of being within reach that may take different dimensions being affordable, timely, frequently mastered, and easy to perform. Quality of surgery relies mostly on adequate human resources (trained and accredited surgical staff and anesthesia professionals) as well as processes optimizing the exploitation of material resources (operating rooms and equipment). Management formalization and checklists will help institutions and surgeons to optimize resources and better adhere to best clinical practice. Image guidance, navigation, and augmented reality should assist surgeons to better deal with frequent patient-specific anatomical variations (personalized care) and master a larger spectrum of diseases as well as better modify strategies on the fly. It is expected but not yet formally demonstrated that image guidance, navigation, and augmented reality assist surgeons in achieving the objectives in line with the Safe Surgery WHO guidelines to avoid excessive blood loss, minimize surgical site infection by reducing open skin intervention time, skin incision size and traction, and potentially improve communication of critical patient information between members of the team. It may also improve efficacy by assisting surgeons to more precisely access the disease, more precisely implant devices or remove diseased tissues. Despite limitations associated with the cost of the equipment and the

P. Bijlenga (✉)
Department of Clinical Neurosciences, Geneva University Hospital and Faculty of Medicine, Geneva University, Geneva, Switzerland
e-mail: philippe.bijlenga@hcuge.ch

M. Jägersberg
Department of Neurosurgery, University of Mainz Medical Center, Mainz, Germany
e-mail: max.jaegersberg@unimedizin-mainz.de

E. Tessitore et al. (eds.), *Surgery of the Cranio-Vertebral Junction*,
https://doi.org/10.1007/978-3-030-18700-2_9

complexity of its handling, image guidance, navigation and augmented reality should soon be widely accessible, accelerate the training learning curve, and broaden the surgical field of each surgeon.

Improving surgical accuracy and safety by means of navigation is of special interest for cervical and craniocervical spine procedures, where demands for precision are extremely high to place long and resilient screws [1]. The anatomical complex relations of the vertebral artery and the spinal cord leave only narrow bony corridors available for screw placement in the lateral masses (C1), the pedicles (C2-C7), articular facets (C1-C2), or the lamina (C2). In many locations, precision tolerances are less than 1 mm in translation and 5° in angulation [2]. Neoplastic, traumatic, or inflammatory diseases alter anatomy and can increase these topographical challenges.

In spite of precision needs, the introduction of navigation for cervical spine procedures had to overcome more obstacles than cranial or lumbar spine surgeries [3]. Accuracy is affected when images are acquired preoperatively and in a different position to that required during the intervention. The size of the operation field, the geometrical access corridors, and size of instruments increase the complexity to optimally position the reference object for accurate navigation during the whole procedure. Constant accuracy checks and registration corrections at the single vertebra scale are considered too time-consuming by many surgeons.

9.2 Definitions

Image-guided surgery is a generic term used to characterize any surgery performed using pre- or intra-operative patient-specific images to guide the operation as opposed to interventions performed according to generic procedures or anatomical landmarks. **Imaging-tracked surgery** are interventions where images are specifically acquired to track the progression of the intervention. A procedure is navigated (**navigated surgery**) when instruments are tracked in real-time and their location and orientation projected on patient-specific pre- or intra-operative acquired images. An operation is performed using **augmented reality (AR)** when images are presented to the surgeon's eye field as a transparent overlay adjusted to the operative field. Augmented reality can be either direct when the surgeons look at the operative field or remote when the operative field and overlays are projected on a screen.

Besides improving the perception of the operating field and overall context, surgery may also be improved by more gentle manipulation of tissues, increased degrees of freedom, precision, and stability of movements that can be provided by robotics. Surgery can be performed as freehand (**freehand surgery**) when surgeons directly manipulate surgical tools or be **robot-assisted** (RAS).

As an example, pedicle screws can be inserted using (1) only anatomical landmarks to identify the entry point and standard reference angles to approximate the insertion trajectory [4, 5]; (2) intra-operative image guidance using a C-arm fluoroscopy to visualize the screw location relative to the bone structures [6]; (3) navigation by tracking the position of the screw relative to a fixed reference previously

registered and by displaying the extrapolated location of the screw relative to earlier acquired images [7]. (4) A virtual semitransparent representation of the vertebra and pedicle is visualized as an overlay on the anatomical structures of the operative field with the optimal entry point and trajectory. The surgeon then inserts the screw following the projected images [3]. (5) A robot is fixed on the spinous process of the targeted vertebra. Two orthogonal fluoroscopic images are acquired including the spine and a reference marker to allow registration with a high-resolution CT scan obtained preoperatively. The screw trajectories are programed, and the robot arm orients a cannula that is used for the drilling. Robot-assisted screw implantation is nowadays frequently used in the lumbar spine but to our knowledge has so far only been tested on cadavers and on a single case regarding cervical spine screws [8, 9].

9.3 Basic Principles

9.3.1 Matching the Resolution and Precision to the Needs

Precision of freehand motion is at best when using microsurgical techniques in the range of one tenth of a millimeter. It is heavily affected by the force to be applied, fatigue, and distance to any pivot point. Visual feedback is essential to allow precise manipulations, and proprioceptive feedback is relevant when the hand or manipulated instrument is out of the visual field. It can be easily experimented performing simple tasks with and without a binocular operative microscope. A normal eye can at best distinguish a 0.07 mm size object. Operative microscopes usually provide a 10× to 60× magnification, reducing the resolution to 1 μm. As a general rule the visual feedback should be 10 times sharper than the required movement precision. The difference between the needed perception resolution and the resulting manipulation precision can be reduced when using micromanipulators or robots. Such a high precision required when operating in the medulla is nevertheless not necessary in most craniocervical surgeries where mechanical constraints are the limiting factors to keep precision within the range of ±0.5 mm and ± 2°.

The precision and limitation of image-guided surgery, navigation, and augmented reality are affected by multiple factors that need to be well understood by the users.

1. Resolution of acquired data set
2. Distortion of the data set, perspective, parallax, special field heterogeneities
3. Co-registration accuracy
4. Structures' motion and deformation

9.3.2 Data Set Acquisition Resolution

The resolution of any imaging data set still remains at least one order of magnitude lower than what can be provided by an operative microscope. The highest resolution

reaches 50 μm when using flat panel detectors but standard thin-sliced CT scan images have a resolution of 0.1 mm, O-arm 0.41 mm in the axial plane, and 0.83 mm in z axis, Ziehm FD Vario 3D 0.375 mm, Arcadis Orbic 3D 0.475 mm, and standard MRI 0.5 mm. The spatial resolution further decreases when using particular imaging protocols such as fiber tracking or functional imaging. The precision of any guidance system will be at best equivalent to the resolution of the most refined data set available. It is therefore recommended to use the data set with the highest resolution as the reference data set to which all others will be registered.

9.3.3 Imaging Distortion

Users need to be aware that 2D images are subject to projection distortions. Most of the intra-operative imaging is acquired using C-arm-mounted fluoroscopic equipment. Here the X-ray source is projecting toward a detector array, and the X-ray beam has a cone shape (Fig. 9.1a). Objects closer to the X-ray source will

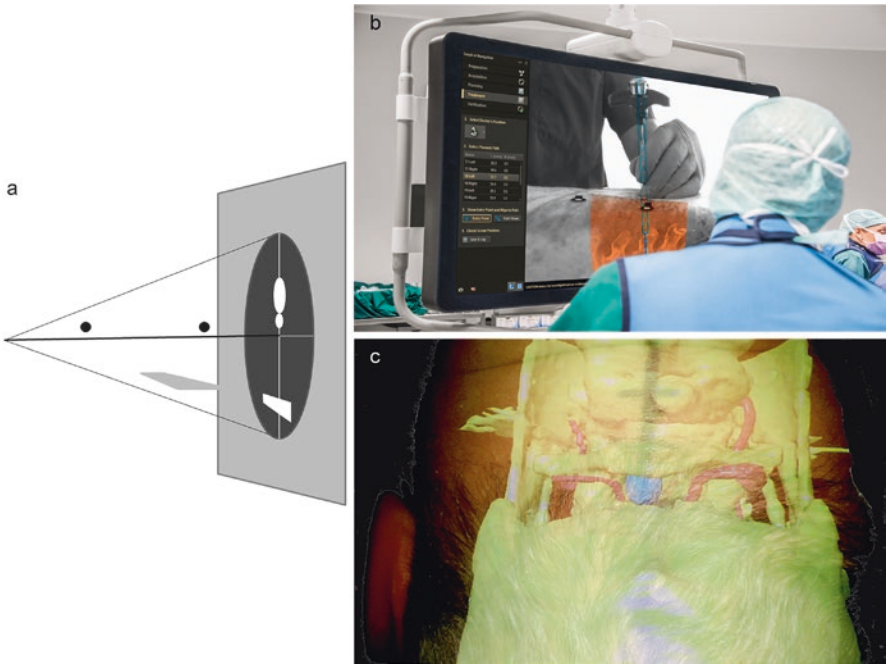

Fig. 9.1 Projection deformation, parallax, and augmented reality. (**a**) Illustration of deformation and relative displacement of objects induced by the projection from a point to a surface. (**b**) Indirect augmented reality. A calibrated video of the intervention field is overlaid on the radiological image (Courtesy Philips Best Netherlands). (**c**) Direct augmented reality. A 3D computer-generated surface rendering of different structures of interest and corresponding to the surgeon's line of sight is projected as an overlay on the microscope head-up display when looking at the patient. Bone is presented in yellow, arteries in red, and lesion in blue

be projected on the detector larger than objects more distant. A surface parallel to the axial beam (beam centered on the source and orthogonal to the detector) will appear progressively more oblique as shifted off center. To minimize errors resulting from inadequate correction of distortion by surgeons, it is recommended to center the axial beam on the target and orient the beam if possible along the surgical axis or as second choice orthogonally. This requires frequent C-arm displacement. Those distortions are avoided when using devices acquiring multiple projections and generating volumetric data displayed as either orthogonal slices or 3D-rendered volumes.

Now, users are faced with another pitfall which is the parallax. Parallax is the apparent relative displacement of objects when viewed from different lines of sight. This commonly tricks surgeons when drawing projections of structures on the surface of the skin. The drawing then only applies when using the line of sight initially used. For deep seated targets, only very small shifts from the initial line of sight can induce great shifts. Errors can be minimized by avoiding to draw on the skin surface and by displaying projections or 3D-rendered image overlays that update continuously for the appropriate line of sight. The overlays can either be projected on a screen and on top of a video image of the operating scene (indirect augmented reality, Fig. 9.1b) or on a head-up display allowing the surgeon to directly look at the operating field and visualize the target as if he could see through the skin of the patient (Fig. 9.1c). Stereoscopic 3D display of the scenery and overlays greatly improve the perception.

Finally users need to be aware that in contrast to X-ray-based imaging, magnetic resonance imaging (MRI) may be significantly distorted because of magnetic field heterogeneities during image acquisition. MRI geometric distortions are reduced as much as possible by calibration and sometimes by imaging post processing. The calibration tolerance for geometrical distortion is less than 2 mm over a 30 cm field of view. When imaging patients, the magnetic field can be extremely deformed (centimeters) by any ferromagnetic object close to the imaging field of view. When head images are acquired, deformation may be induced by ferromagnetic dental material, ventriculoperitoneal shunt valves, or clips. Earrings and piercings, another common source of imaging distortion, are normally removed before performing imaging.

9.3.4 Registration Accuracy

The co-registration accuracy may be affected at multiple levels, but the most vulnerable step is the physical co-registration of the patient with the virtual model when performing a navigated intervention. Navigation relies on recording the relative position of points (identified both on the surface of the skin of the patient and in the virtual model) according to a reference object visible to the navigation system. Most frequently this co-registration process is performed using multiple points to surface-matching the exposed vertebrae. This technique is rapid, easy, and reliable for standard patients positioned in prone decubitus.

The development of intra-operative imaging has helped to overcome some of the registration shortcomings. Based on fluoroscopy, intra-operative imaging acquisition is performed after surgical exposure with the navigation reference-object in position. Initially based on orthogonal 2D image acquisitions, progress in engineering led to the development of devices that isocentrically rotate around the patient. Such devices allow the reconstruction of 3D data sets from images acquired in multiple projections (O-Arm, Medtronic Surgical Technologies, Louisville, USA; Airo Mobile Intraoperative CT, Brainlab, Munich, Germany; Ziehm FD Vario 3D, Ziehm Imaging GmbH, Nuremberg, Germany; Arcadis Orbic 3D, Siemens Medical Solutions, Erlangen, Germany; see Fig. 9.2). 3D navigation of instruments can hence be used immediately without further accuracy-decreasing point matching (StealthStation, Medtronic Surgical Technologies, Louisville, USA; VectorVision^2, Brainlab, Munich, Germany). The gain in precision derived from this in situ and navigation-referenced acquisition allows fixing a larger reference object via an attachment to the head holder instead of a clamp fixed on cervical bone. It reduces the problem of interference between surgical and navigation instruments.

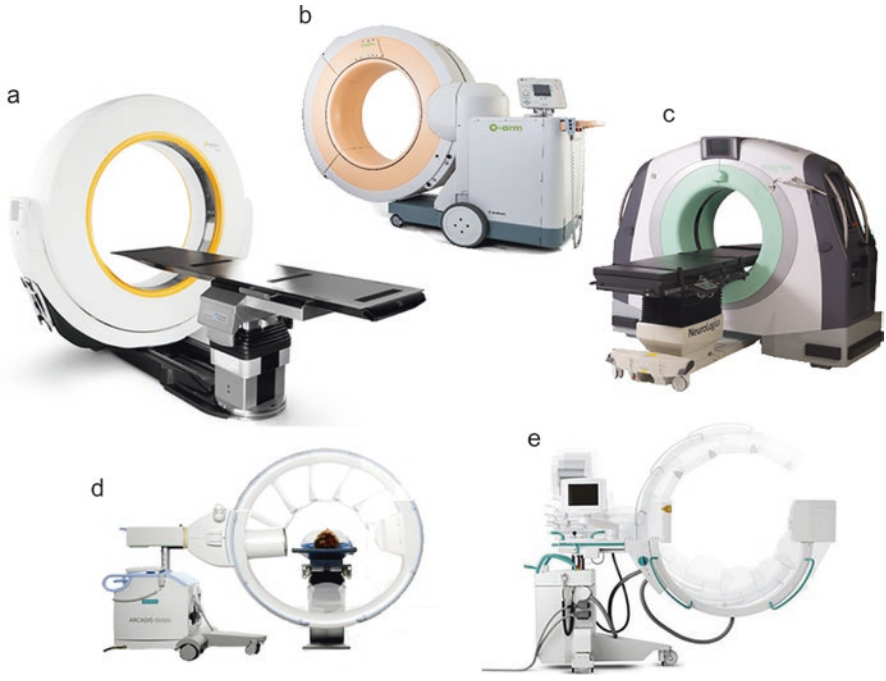

Fig. 9.2 Mobile intra-operative imaging devices currently available. (**a**) Airo Mobile Intraoperative CT, BrainLAB, München, Germany; (**b**) O-Arm, Medtronic Surgical Technologies, Louisville, USA; (**c**) BodyTom®, NeuroLogica Samsung, Danvers, USA; (**d**) Arcadis Orbic 3D, Siemens Medical Solutions, Erlangen, Germany; (**e**) Ziehm FD Vario 3D, Ziehm Imaging GmbH, Nuremberg, Germany

The accuracy of the registration may be affected by the distance between the reference object and the navigation camera, as well as by the distance between the reference object and the operating field. To improve accuracy, distances should be minimized. The reference object should be placed as close as possible to the operating field but should not disturb or enter in collision with instruments. It should be avoided placing the reference object between the surgeon and the scrub nurse. The maximum recommended distance between the operating field and the reference object should be below 30 cm. The identification of navigated instruments and of the reference object and their relative positions are calculated based on relative angle measurements between infrared-reflecting fiducials fixed on the objects and detected by two stereoscopic cameras. The optimal distance is usually between 1.5 and 2 m. Most of the systems use infrared light sources and camera and require direct line of sight between cameras, reference object, and instruments.

Some navigation systems use electromagnetic field generators to localize instruments. Those systems do not require line of sight. They allow not only to track the instrument as a rigid object but also to track the tip of flexible tools like stylets and catheters. A drawback that users have to be aware of is that the electromagnetic field may be distorted by other sources of electromagnetic fields such as coagulation generators or ferromagnetic objects.

The registration process is a major step subject to the highest risk of inaccuracy. It is therefore mandatory to check the accuracy. Most navigation systems prompt surgeons to point on easily identifiable structures on both sides of the patient to check the overall orientation and accuracy.

Using augmented reality, the microscope or head-up display need to be registered and calibrated. It is then easy to verify the overall registration accuracy by projecting a model of the patient's skin surface on the head-up display and verify the perfect adjustment of the model with reality (Fig. 9.3). It is recommended to check the registration accuracy at least in two planes, typically the coronal plane using the face (nose, eyes, and eyebrow) and the sagittal plane using the nose and ears. In prone position, mastoid processes and ears as well as the inion and upper neck skinfolds may be used.

Once the registration accuracy is checked, it is recommended to mark four points and record their position with the navigation system in case either the reference object or the patient is inadvertently moved during draping, trephination, or drilling. This process can be repeated when bone is exposed. Four small holes can be drilled just to allow the tip of the pointer to be stabilized. This is the most accurate method to verify the registration all along the procedure.

9.3.5 Structures' Motion and Deformations

When working on soft tissues or on the spine, structures may move. It is unlikely that the patient will lie in the operating room exactly in the same position as during imaging acquisition. Furthermore manipulations during the operation will most probably change the relative position of mobile structures of interest. During

Fig. 9.3 Co-registration accuracy check. The accuracy of the registration process is verified by visually assessing how the virtual model of the patient head (blue) matches the real anatomy. If the patient's face is accessible, the nose (lateral registration and sagittal plane rotation assessment) and forehead (vertical registration and axial plane rotation assessment) are excellent landmarks. The depth registration (anteroposterior registration and coronal plane rotation assessment) is verified by scanning up and down, visualizing the plane of focus moving over the facial 3D anatomy (upper left and right). In prone position the ear anatomy, the mastoid, and the inion are the major landmarks. Care must be taken during image acquisition to avoid excessive deformation of the concha when immobilizing the patient's head

cerebral surgery, removal of craniospinal fluid, opening of fissures, and resection of tissue may lead to brain shifts ranging up to tens of millimeter. In the craniocervical junction C0-C1 and C1-C2 may rotate by 15° each in the flexion/extension axis and a few degrees in lateral flexion but up to 70° between C1 and C2 in rotation. Errors due to structure motion can be prevented by repeating registration for each mobile structure.

During spine surgery navigation based on preoperative imaging, it is recommended to fix the reference object on the spinous process of the vertebra that will be operated on to maximize precision. When performing cervical spine surgery, navigation based on intra-operative imaging, a metallic head holder, and head holder table attachment provide better fixation than radiolucent head holder systems and can be used without problematic radiologic artifacts if placed with a rostral angle [10]. Care must be taken that the attachment of the head holder to the table allows the required space for the applied radiologic device allowing the cervical spine to be placed into the C-arm iso-center (see Fig. 9.4). Table systems allowing the head fixation from the rostral table extremity (e.g. Jackson Table System, Mizuho OSI, Union City, USA; Maquet Alphamax with extension, Maquet Cardiovascular LLC, New Jersey, USA) are advantageous but not mandatory. The acquisition should be performed under apnea and with the wound retractors left in situ since their repositioning can alter the positions between vertebrae [11]. The wound cavity should be filled with saline solution to enhance image quality.

If avoidable, the operation table should not be moved until instrumentation is accomplished. Other movements that can alter intervertebral position must be avoided or left to the end of the procedure. It is hence suggested that entry points and pressure-free trajectory drilling should be accomplished for all planned screws before tapping and screw placing is performed. It is advantageous to start the procedure at the most caudal vertebra which has the greatest distance to the reference arc

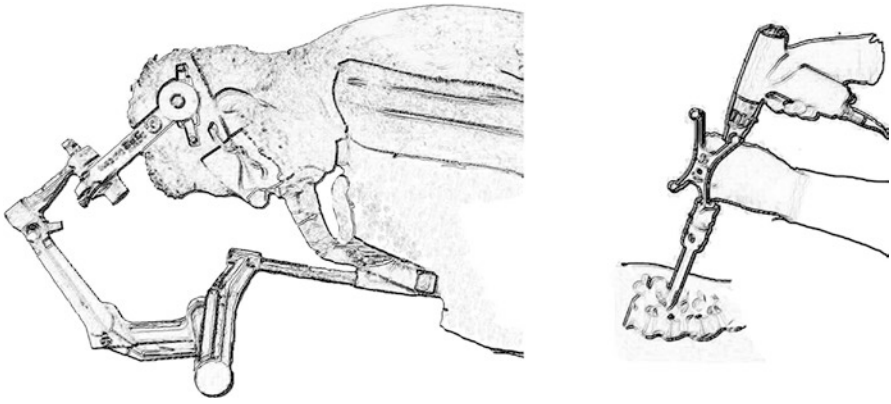

Fig. 9.4 Specific equipment and adjustments to optimize craniocervical junction surgeries using intra-operative imaging and navigation. Positioning of the patient, head clamp, and support extension (left). Navigated drill guide (right)

and to advance in the rostral direction, this way the increasing loss of precision with surgery time is not adding to the loss of precision due to distance to the reference arc. The use of a navigated drill guide (Fig. 9.4) is recommended in order to reduce pressure on the vertebrae. Then, a bone trajectory is performed with a 2.7 or 2.9 mm drill which is inserted through the guide. A screw is then inserted following a k-wire into the performed trajectory. If occipital fixation is necessary, these screws will accordingly be the last screws to place, since the reference arc is directly fixed to C0, and since these screws do not require precise navigation.

An analogous setup can be used for anterior instrumentation in the supine position; however, usually only one type of screw, the odontoid screw, is of interest for navigation, and not all considerations mentioned above are hence of importance for this surgery [12].

Augmented reality allows a better perception and correction by surgeons of inadvertent displacement of structures from original position. When using augmented reality, it is recommended to segment each mobile structure that could be used as a reference and all target structures. It is then easy for the surgeon to see how well the reference structure fits the projected overlay model, correct for the misalignment, and extrapolate where the target structure or desired trajectory is. The process of local registration using a reference structure is crucial for precise navigation at the millimetric scale which is important when operating in the craniocervical junction. The process is illustrated in the case description below.

9.4 Spinal Navigation: Current Status

The majority of studies about spinal navigation and implant accuracy address the lumbar spine, and misplacement classification systems (e.g., the often-mentioned Gertzbein-Robins classification [13]) have the shortcoming that their thresholds have been chosen with regard to lumbar spine morphometry and respective tolerances. Some authors consider minor misplacements (up to 2 mm or grade 1 according to Gertzbein-Robins) as correctly placed screws for lumbar accuracy analysis. In contrast, cervical spine pedicle screw misplacements of 2 mm in any direction could already cause damage. Some authors therefore apply a misplacement classification of “screw exposure” (less than 50% of the screw outside the pedicle) and “pedicle perforation” (more than 50% of the screw outside the pedicle) for the cervical spine which is more suitable in the context of this delicate anatomy.

Several meta-analyses report the rates of (mainly lumbar) screw misplacements with or without navigation and show an advantage using spinal navigation. Mason et al. analyzed 30 publications including 1973 patients in whom 9310 pedicle screws were inserted. With conventional fluoroscopy, 2D fluoroscopic navigation, and 3D fluoroscopic navigation, accuracy (absence of pedicle wall breaches) of 68.1%, 84.3%, and 95.5% was respectively achieved [14]. Tian et al. showed similar results in their meta-analysis of 43 studies [15].

In the cervical spine, special interest for navigation addresses the placement of pedicle screws in subaxial levels C3-C6. These screws are far more resilient than the less challenging lateral mass screws, but highest possible precision is crucial because of the challenging pedicle dimensions immediately adjacent to sensitive neurovascular structures. Yukawa et al. reports a series of fluoroscopy assisted insertions of 620 cervical pedicle screws with 3.9% (95%CI 2.5% to 5.8%) rate of perforation (>50% of screw outside pedicle) and 9.2% (95%CI 7% to 12%) rate of "screw exposure" (<50% of screw outside pedicle) [16]. Abumi et al. report a cervical screw misplacement rate of 4.7% with conventional fluoroscopy in their collective of 26 patients [17]. A multicenter study led by Nagoya University and including 84 patients reports a rate of screw exposure of 15.4% and pedicle perforation of 4.1% [18]. Richter et al. prospectively enrolled 52 patients in their comparative study and observed 8.6% and 3% for conventional and navigated surgery, respectively [19]. Using spinal navigation, according to Kotani et al., the misplacement rate can be reduced to 1.2% [20]. On the other hand, Uehara et al. who analyzed the misplacement rates in their collective of 359 patients along the cervical to lumbar spine, all operated under navigation, report higher misplacement rates, especially of subaxial pedicle screws (5.0% for C2, 11.4% for C3–5, and 7.0% for C6–7, [21]). Lateral mass screws in C1 and pars screws in C2 are less critical when placed conventionally under fluoroscopy. Tessitore et al. who analyzed 111 of these screws found 3% misplacement, all less than 2 mm [22]. Those rates increase in the presence of anatomy-altering disease [21, 23]. Misplacement, including "screw exposures," can potentially cause devastating complications in the cervical spine. The cited data shows that accuracy improvement by means of navigation significantly lowers the risk of screw misplacement and thereby enhances patient safety.

Furthermore, 3D navigation device has been used to safely insert odontoid screws in case of dens fracture [12, 24]. Another valuable advantage in the intraoperative 3D radiological control of implants is the possibility to correct misplaced screws within the same session. Finally, the exposure of surgical teams to irradiation is drastically reduced [25, 26].

9.5 Case Description

A 78-year-old patient complaining of neck pain, limited motion when turning the head clockwise, and long-lasting right-sided headaches sought medical advice. An unsuccessful infiltration of the second cervical nerve on the right side was performed. The patient then benefitted of a head and neck magnetic resonance imaging that led to the discovery of a right-sided and anterior intradural extramedullary cystic lesion at the craniocervical junction typical of a neuro-enteric cyst. A resection of the lesion was recommended to the patient.

A CT scan of the cervical spine was obtained. T2-weighted MRI images 1.4 mm in thickness, time-of-flight (TOF) sequence 1.2 mm in thickness, and bone

windowed CT scan images 1.25 mm in thickness were merged and fused on the navigation planning station (iPlan Netnet®, Brainlab, Germany). Virtual objects were segmented using gray scale thresholding. The skin surface of the head and the bone surface of the skull and vertebra were segmented from the CT scan, the vertebral arteries from the TOF imaging, the brain stem, and medulla from the T2 MRI imaging (Fig. 9.5).

The patient was installed in prone position and the head fixed in a head clamp. The reference stars with reflecting fiducials were fixed on the head holder and microscope. The patient's position was registered using skin surface matching with the Softouch® (Brainlab, Germany) starting with the guide option using both lateral canthus and inion and then multiple points on both lateral aspects of the perioccular skin surface and both concha cymba and cavum as well as mastoid processes. The microscope calibration was checked and recalibrated on the reference star as a standard procedure. Both microscope and patient registration were checked by projecting the virtual head skin surface on the real patient using the microscope head-up display and orienting the microscope. The microscope was first oriented perpendicular to the sagittal plan and aiming toward the ears both sides to capture possible mismatches in the superoinferior and anteroposterior axis and finally perpendicular to the coronal plan and aiming to the inion to

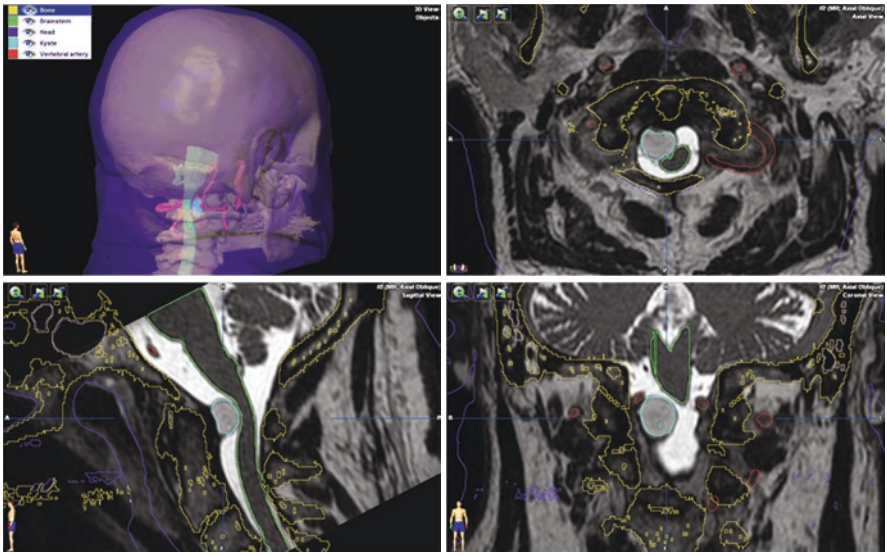

Fig. 9.5 Neuronavigation screenshot illustrating segmented objects: skin surface of the patient's head (blue), bone (yellow), brainstem (green), arteries (red), and lesion (light blue). 3D semitransparent surface rendering projection (upper left), axial slice (upper right), sagittal plane (lower left), and coronal plane (lower right)

capture possible mismatches in the lateral axis and superoinferior axis on the midline (Fig. 9.3).

Once the accuracy was checked, the bone structures, vertebral arteries, the cyst, and the medulla were projected as overlays on the head-up display and the optimal intervention trajectory defined. Skin incision was drawn on the skin accordingly.

After exposure of the skull and C1 vertebra the virtual bone surface was overlaid in the microscope head-up display to verify the accuracy of the registration, and no significant displacement of the vertebra was induced by the patient positioning. If displacements are noticed, local point-based registrations on the bone surface can be performed. The vertebral artery was then projected to be formally localized before proceeding to the C1 vertebra drilling (Fig. 9.6a, b).

Once the C1 right-sided lamina and inferior aspect of the foramen magnum were drilled, the accuracy of the registration was assessed again and the cyst and medulla were projected before dura opening (Fig. 9.6c, d).

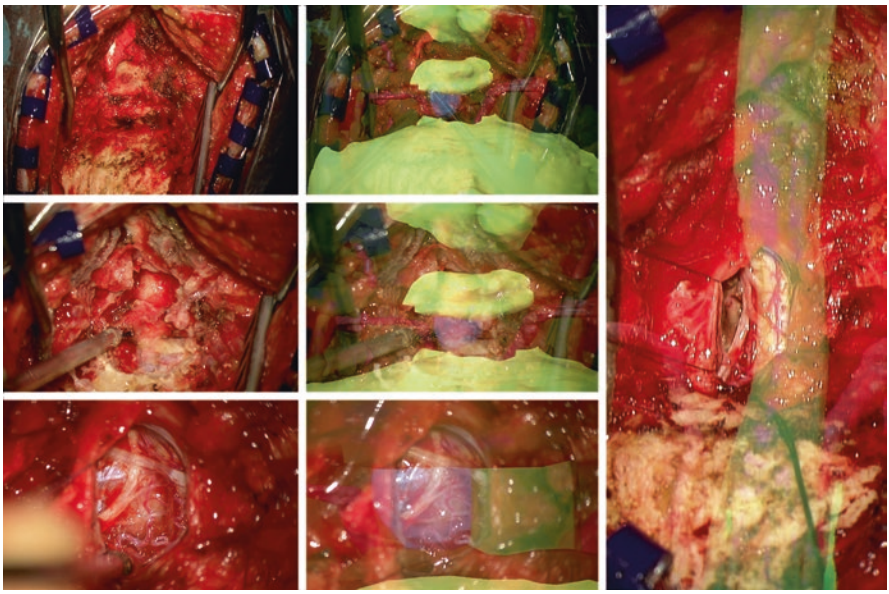

Fig. 9.6 Case illustration. Surgical field photographs without augmented reality taken before the drilling of C1 (upper left), before dura opening (middle left), before lesion resection (lower left), and with the addition of augmented reality (middle column). Surgical field overview illustration after lesion removal with the addition of augmented reality illustrating the deformation of the medulla. Notice how augmented reality facilitates the identification of the vertebral artery, how the anatomy is perfectly matched prior to the drilling, and how it has to be checked and corrected prior to dura opening (vertical shift induced by the pressure of the drill on the lamina)

After dura opening, the location of the cyst and medulla were confirmed by the projection of the virtual objects (Fig. 9.6e, f). Complete cyst removal was achieved laterally, and the most medial aspect of the cyst basis on the anterior aspect of the dura was coagulated. The overlap of the virtual and real medulla and its deformation by the cyst is illustrated (Fig. 9.6g).

9.6 Perspectives

For the purpose of demonstration, a pointer was positioned on the trajectory of a potential screw to be inserted in the C2 lateral mass on the right side and the projection in the head-up display switched to the 2D view. The image visualized corresponds to the CT scan image slice orthogonal to the optic axis of the microscope at the level of the microscope focus plane. The green cross shows the extended pointer tip and the line of the pointer trajectory. Here the surgeon can scan up and down using the focus to visualize all the structures along the pointer trajectory. Surgeons have two visualization options: either a semitransparent 3D representation of structures or a 2D image scrawling along the surgical path. Both views are complementary for a better understanding of the anatomy (Fig. 9.7).

In the future, computer vision and automatic anatomical co-registration should allow to avoid the use of the navigation cameras and reference objects. It should allow very accurate registration using marks (methylene blue marking of bone edges or other type of marks) to be aligned with the contour lines of the bone or vessels (Fig. 9.8). Direct image-based registration should allow accurate and updated 3D augmented reality overlays using the microscope or protection glasses avoiding most of the pitfalls and cumbersome registration and checks currently needed.

Such assistance, associated with continuous and regular education, regular practice, case-specific preparation, and formalizing each step from initial evaluation to final assessment using structured care pathways, may both increase efficiency and quality.

Fig. 9.7 Perspective using augmented reality for screw insertion. The stereoscopic image of the skull and cervical spine is projected in the microscope head-up display. A pointer is used to identify the entry point and trajectory angle (upper inset). The surgeon switches to a 2D representation of the imaging showing a slice orthogonal to the line of sight at the level of the focus plane. The surgeon can easily scan up and down to visualize the relationship between the trajectory path and surrounding structures. The trajectory is expanded from the skin to the depth using the tip extension tool. The green cross shows the tip of the pointer. The red cross shows the tip of the virtual extension located in the middle of the pedicle and in the focal plane (middle insert). 3D volume rendering projection of the structures with planned trajectory. The surgeon can adjust the pointer orientation to the optimal trajectory and check the accuracy by verifying the collocation of the virtual image of the spinous processes of C1 and C2 with their actual location by palpation (lower inset)

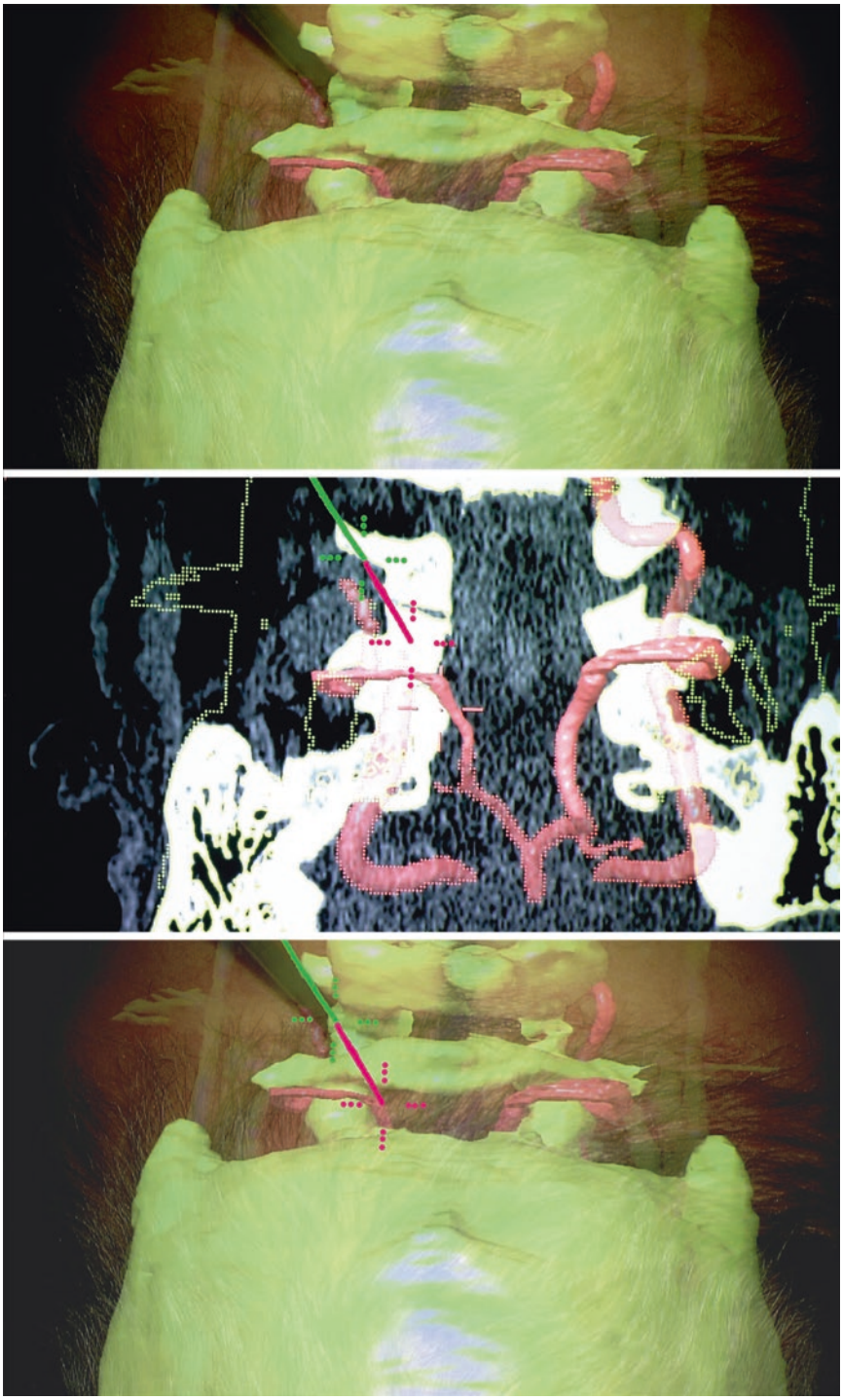

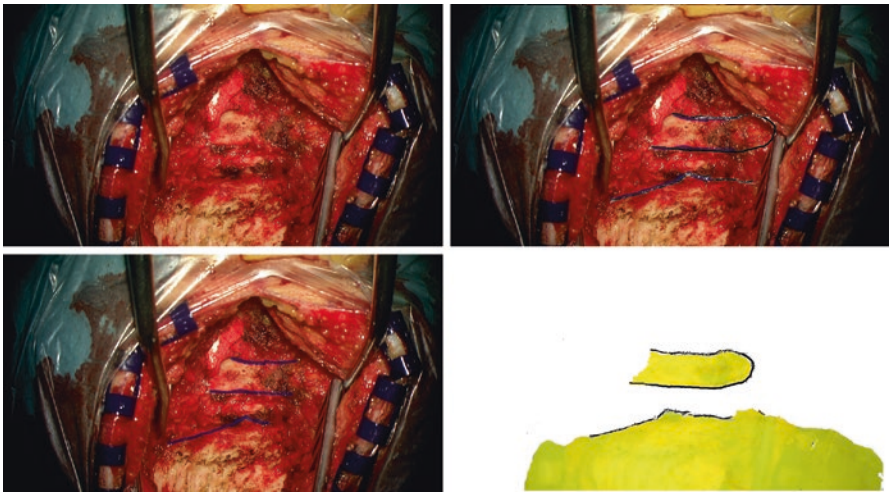

Fig. 9.8 Example of possible solution to facilitate image-based re-registration and computer vision life registration correction. Signature bone edges are identified from the computer reconstruction of the operative field (lower right). The signature bone edges are exposed in the operative field (upper left) and marked using methylene blue ink (lower left). The computer adjusts the virtual image to reality by overlapping the signature shape of the calculated bone edges with the methylene blue marking. Vertebra and skull being independent objects with specific signature edges, the computer should be able to track and correct for relative motion of different rigid objects

Acknowledgments I would like to thank Nadja Heindl and Valentin Elefteriu for their careful review of the manuscript.

References

1. Ogihara N, et al. Long-term results of computer-assisted posterior occipitocervical reconstruction. World Neurosurg. 2010;73(6):722–8.
2. Rampersaud YR, Simon DA, Foley KT. Accuracy requirements for image-guided spinal pedicle screw placement. Spine (Phila Pa 1976). 2001;26(4):352–9.
3. Elmi-Terander A, et al. Surgical navigation technology based on augmented reality and integrated 3D intraoperative imaging: a spine cadaveric feasibility and accuracy study. Spine (Phila Pa 1976). 2016;41(21):E1303–11.
4. King D. Internal fixation for lumbosacral fusion. J Bone Joint Surg Am. 1948;30A(3):560–5.
5. Roy-Camille R, Saillant G, Mazel C. Internal fixation of the lumbar spine with pedicle screw plating. Clin Orthop Relat Res. 1986;(203):7–17.
6. Odgers CJt, et al. Accuracy of pedicle screw placement with the assistance of lateral plain radiography. J Spinal Disord. 1996;9(4):334–8.
7. Kalfas IH, et al. Application of frameless stereotaxy to pedicle screw fixation of the spine. J Neurosurg. 1995;83(4):641–7.
8. Tian W. Robot-assisted posterior C1–2 transarticular screw fixation for atlantoaxial instability: a case report. Spine (Phila Pa 1976). 2016;41(Suppl 19):B2–5.
9. Kostrzewski S, et al. Robotic system for cervical spine surgery. Int J Med Robot. 2012;8(2):184–90.

10. Nottmeier EW, Young PM. Image-guided placement of occipitocervical instrumentation using a reference arc attached to the headholder. Neurosurgery. 2010;66(3 Suppl Operative):138–42.
11. Guppy KH, Chakrabarti I, Banerjee A. The use of intraoperative navigation for complex upper cervical spine surgery. Neurosurg Focus. 2014;36(3):E5.
12. Pisapia JM, et al. Navigated odontoid screw placement using the O-arm: technical note and case series. J Neurosurg Spine. 2017;26(1):10–8.
13. Gertzbein SD, Robbins SE. Accuracy of pedicular screw placement in vivo. Spine (Phila Pa 1976). 1990;15(1):11–4.
14. Mason A, et al. The accuracy of pedicle screw placement using intraoperative image guidance systems. J Neurosurg Spine. 2014;20(2):196–203.
15. Tian NF, et al. Pedicle screw insertion accuracy with different assisted methods: a systematic review and meta-analysis of comparative studies. Eur Spine J. 2011;20(6):846–59.
16. Yukawa Y, et al. Cervical pedicle screw fixation in 100 cases of unstable cervical injuries: pedicle axis views obtained using fluoroscopy. J Neurosurg Spine. 2006;5(6):488–93.
17. Abumi K, et al. Posterior occipitocervical reconstruction using cervical pedicle screws and plate-rod systems. Spine (Phila Pa 1976). 1999;24(14):1425–34.
18. Nakashima H, et al. Complications of cervical pedicle screw fixation for nontraumatic lesions: a multicenter study of 84 patients. J Neurosurg Spine. 2012;16(3):238–47.
19. Richter M, Cakir B, Schmidt R. Cervical pedicle screws: conventional versus computer-assisted placement of cannulated screws. Spine (Phila Pa 1976). 2005;30(20):2280–7.
20. Kotani Y, et al. Improved accuracy of computer-assisted cervical pedicle screw insertion. J Neurosurg. 2003;99(3 Suppl):257–63.
21. Uehara M, et al. Screw perforation rates in 359 consecutive patients receiving computer-guided pedicle screw insertion along the cervical to lumbar spine. Eur Spine J. 2017;26(11):2858–64.
22. Tessitore E, et al. Accuracy of freehand fluoroscopy-guided placement of C1 lateral mass and C2 isthmic screws in atlanto-axial instability. Acta Neurochir. 2011;153(7):1417–25; discussion 1425.
23. Uehara M, et al. Perforation rates of cervical pedicle screw insertion by disease and vertebral level. Open Orthop J. 2010;4:142–6.
24. Zou D, et al. Three-dimensional image navigation system-assisted anterior cervical screw fixation for treatment of acute odontoid fracture. Int J Clin Exp Med. 2014;7(11):4332–6.
25. Mendelsohn D, et al. Patient and surgeon radiation exposure during spinal instrumentation using intraoperative computed tomography-based navigation. Spine J. 2016;16(3):343–54.
26. Villard J, et al. Radiation exposure to the surgeon and the patient during posterior lumbar spinal instrumentation: a prospective randomized comparison of navigated versus non-navigated freehand techniques. Spine (Phila Pa 1976). 2014;39(13):1004–9.